Heliyon 10 (2024) e31904

Contents lists available at ScienceDirect

Heliyon

journal homepage: www.cell.com/heliyon

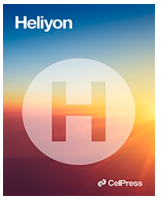

Research article

Methodology exploration and reproducibility evaluation of TAI and TSI for quantitative ultrasound assessment of hepatic steatosis

Xiao Li [a,1], Ziwei Sun [a,1], Wei Liu [a,1], Lianjie Sun [b], Junyi Ren [a], Ying Xu [a], Haoyong Yu [c,**], Wenkun Bai [d,*]

[a] *Department of Ultrasound in Medicine, Shanghai Sixth People's Hospital Affiliated to Shanghai Jiao Tong University School of Medicine, Shanghai, China*

[b] *Qingdao University, Qingdao, China*

[c] *Department of Endocrinology and Metabolism, Shanghai Sixth People's Hospital Affiliated to Shanghai Jiao Tong University School of Medicine, Institute of Shanghai Diabetes, Shanghai, China*

[d] *Department of Ultrasound in Medicine, Tongji Hospital Affiliated to Tongji University, Shanghai Institute of Ultrasound in Medicine, Shanghai, China*

A R T I C L E I N F O

Keywords:
Metabolic dysfunction-associated steatotic liver disease
Quantitative ultrasound
Controlled attenuation parameter
Tissue attenuation imaging
Tissue scatter distribution imaging

A B S T R A C T

Background and aim: New quantitative ultrasound techniques can be used to quantify hepatic steatosis, including tissue attenuation imaging (TAI), tissue scatter -distribution imaging (TSI), and the hepatorenal index (HRI). However, the measurement norms and the effects of fasting on these measurements remain unclear. The present study performed a methodological exploration and investigated the reliability of these measurements.

Methods: In total, 103 participants were prospectively recruited for ultrasonography and magnetic resonance imaging (MRI) scans. For the TAI and TSI data, the upper (2 cm), middle (4 cm) and lower (6 cm) areas determined according to the depth of the region of interest from the liver capsule, were sampled three times. Correlation analyses were performed to compare the measurements of TAI, TSI, and HRI with the controlled attenuation parameter (CAP) or MRI-proton density fat fraction (MRI-PDFF). Intra- and inter-operator repeatability was assessed using intraclass correlation coefficients. The effects of fasting on these measurements were then compared.

Results: The TAI and TSI measurements obtained from the upper and middle depths exhibited stronger correlations with the CAP measurements than those obtained from the lower depth. Specifically, the mean TAI had a significant positive correlation with MRI-PDFF ($r = 0.753$, $P < 0.0001$). TAI and TSI measurements exhibited excellent intra- (0.933 and 0.925, respectively) and inter- (0.896 and 0.766, respectively) examiner reliability. However, the correlation between HRI and CAP measurements was only 0.281, with no significant correlation with MRI-PDFF, and intra- and inter-examiner reproducibility of 0.458 and 0.343, respectively. Fasting did not affect these measurements.

* Corresponding author. Department of Ultrasound in Medicine, Tongji Hospital Affiliated to Tongji University, Shanghai Institute of Ultrasound in Medicine, Shanghai, China

** Corresponding author. Department of Endocrinology and Metabolism, Shanghai Sixth People's Hospital Affiliated to Shanghai Jiao Tong University School of Medicine, Yishan Road 600, Shanghai, 200233, China

E-mail addresses: yuhaoyong111@sjtu.edu.cn (H. Yu), doctor505@alumni.sjtu.edu.cn (W. Bai).

[1] These authors contributed equally.

https://doi.org/10.1016/j.heliyon.2024.e31904
Received 26 April 2023; Received in revised form 23 May 2024; Accepted 23 May 2024
Available online 24 May 2024

Conclusions: TAI and TSI measurements demonstrated good intra- and interobserver reliability and correlated well with CAP and MRI-PDFF measurements. However, in practice-based clinical applications, the sampling depth should be controlled within 2–4 cm of the hepatic capsule; no fasting is required before the examination.

1. Introduction

Metabolic dysfunction-associated steatotic liver disease (MASLD) is a major global health concern, with an increasing prevalence of fatty liver disease related to systemic metabolic dysregulation [1]. Pathological changes in MASLD may include simple fatty liver or non-alcoholic steatohepatitis with or without liver fibrosis [2]. The latter two are relatively reversible but not when the disease progresses to cirrhosis. Therefore, early screening and monitoring of MASLD are crucial.

Percutaneous liver biopsy remains the gold standard technique for diagnosing hepatic steatosis; however, it carries risks of invasive complications, sampling errors, and diagnostic subjectivity. Therefore, reliable non-invasive tools for diagnosing hepatic steatosis are urgently needed [3]. Magnetic resonance imaging-proton density fat fraction (MRI-PDFF) can accurately quantify liver fat with high sensitivity and specificity and good repeatability and reproducibility [4]. However, this approach is not ideal for screening large at-risk populations. Ultrasound (US) is an essential first-line imaging modality for patients with MASLD. Conventional B-mode US is based mainly on a subjective qualitative evaluation of the internal echo of the liver parenchyma and is currently widely used in clinical screening for fatty liver [5]. However, it cannot be used as a reliable and accurate diagnostic tool because of its insufficient objectivity, dependence on operator experience, tendency for interobserver variability, and poor sensitivity in diagnosing mild fatty liver. Quantitative US (QUS)-based imaging techniques have substantially improved the detection and quantification of hepatic steatosis. Controlled attenuation parameters (CAP) determination using transient elastography is an effective tool for quantitatively assessing of fatty liver infiltration [6]. In a study involving 1771 patients who underwent liver biopsies, CAP demonstrated good sensitivity and specificity in distinguishing stages 1, 2, and 3 of hepatic steatosis [7]. The measurement area for CAP was significantly larger than that for liver biopsy, reducing the potential risk for sampling bias. However, measurements are obtained without visualization of the liver and, as such coincide with masses, vessels, or heterogeneous steatosis, leading to false-positive or false-negative results.

New visual QUS diagnostic tools have demonstrated advantages in hepatic steatosis evaluation. QUS uses tissue scattering imaging (TSI) and tissue attenuation imaging (TAI) of the liver parenchyma for objective quantitative evaluation and has demonstrated good diagnostic performance in predicting hepatic steatosis [8]. TAI measures echo attenuation in tissues and calculates the attenuation coefficient (AC) in dB/cm/MHz. TSI measures echo backscatter using speckle statistics and calculates the scattering coefficient (SC) [9–11]. Another semiquantitative measurement based on an artificial intelligence algorithm, known as EzHRI, yields the hepatorenal index (HRI) using histogram analysis comparing the echo amplitudes between the liver parenchyma and renal cortex [12]. All three of these new techniques are used to assess hepatic steatosis. Previous studies have demonstrated good diagnostic performance in detecting hepatic steatosis and good intra- and interobserver reliability in a single examination [10,11,13]. However, the influencing factors in more complex, real-world settings, including differences in patient status and operating practices, have not yet been studied.

The measurement results of TAI and TSI demonstrate high repeatability, however, different sampling depths significantly affect these results. Presently, there are many measurement methods; however, the sampling depths vary (at least 1 cm, 3–4 cm, 4–8 cm, etc.) [8,14,15]. We evaluated the measurements at different sampling depths commonly used in clinics to determine the most reliable operating standard. Additionally, the effect of fasting on these measurements is inconclusive. Studies have suggested that liver congestion, elevated levels of liver enzymes and bilirubin, and biliary obstruction affect liver elasticity and may lead to false-positive results. However, other studies have found that fasting does not affect CAP measurements [16]. Ratchatasettakul et al. reported that CAP decreased significantly after ingesting a liquid meal (15–120 min) and returned to fasting levels after 150 min [17]. The present study also investigated the differences in QUS and CAP measurements between fasting and 2 h postprandial conditions.

Current clinical studies exist investigating the feasibility and repeatability of evaluating hepatic steatosis based on TAI and TSI; however, there is a lack of uniform operating standards. As such, this study attempted to conduct a methodological discussion, design a relatively complete comparison method, evaluate the measurement accuracy and repeatability of different sampling depths, compare intra- and interclass differences, and determine the correlation between CAP measurements and MRI-PDFF scans to find the most reliable measurement standard to provide a reference for the standardized clinical application of QUS.

2. Materials

2.1. Study participants and selection criteria

Patients with confirmed or suspected MASLD who visited the endocrinology department of our hospital and healthy volunteers (apparently healthy employees or students without known liver disease) were prospectively recruited from October 2022 to December 2022. Participants voluntarily underwent abdominal US examination and quantitative liver fat content measurements. The exclusion criteria were as follows: history of liver surgery, liver tumors, obstructive cholestasis, right heart failure or liver congestion, current treatment with radiotherapy or chemotherapy for malignant tumors, and significant alcohol consumption, defined as 14 and 21 standard drinks per week for women and men, respectively. Volunteers underwent CAP and MRI-PDFF scanning once and US scanning three times in one week. US examinations of the selected participants were performed without compensation. A flow diagram

illustrating the study design is presented in Fig. 1.

A total of 103 participants were included in this study, of whom 40 underwent MRI-PDFF. Dyslipidemia was defined according to the National Cholesterol Education Program Adult Treatment Panel III (NCEP ATP III) diagnostic standard (with ≥ of the following): total cholesterol ≥6.21 mmol/L; high-density lipoprotein <1.03 mmol/L; low-density lipoprotein ≥4.16 mmol/L; and triglycerides ≥2.26 mmol/L [18]. Hypertension was defined as a blood pressure >140/90 mmHg, according to the 2018 European Society of Cardiology (ESC)/European Society of Hypertension (ESH) guidelines [19]. Criteria for the diagnosis of diabetes were fasting blood glucose (FBG) ≥ 7.0 mmol/L or 2 h plasma glucose ≥11.1 mmol/L during a 75 g oral glucose tolerance test, glycated hemoglobin (HbA1c) ≥ 6.5 %, classic symptoms of hyperglycemia or hyperglycemic crisis, or random plasma glucose ≥11.1 mmol/L [20].

This study strictly complied with the ethical requirements of biomedical research published by international and domestic organizations. The Medical Ethics Committee of our hospital approved this prospective study (Ethics Approval Number 2021-KY-025[K]), and written informed consent was obtained from all patients.

2.2. CAP measurement

For each participant, CAP scanning was performed using the FibroScan system (Echosens, Paris, France) equipped with an L probe by a dedicated technician with three years of experience. The operator was blinded to the clinical and biological information of the participants. During the examination, participants were positioned supine with their right hand raised and rib cages spread. The probe was placed vertically on the skin surface between the 9th and 11th intercostal spaces adjacent to the right lobe of the liver on the midaxillary or anterior axillary line [21]. The detection range of the liver was 2.5–6.5 cm below the skin, and there were no large blood vessel structures. The ratio of the interquartile range (IQR) to the median value (M) of the CAP was calculated to evaluate variability. At least ten successful acquisitions were obtained for each subject. The measurement was reliable if the IQR/M ratio of the CAP obtained from ten valid acquisitions was ≤0.3 [22,23]. Participants were grouped based on CAP values, as follows: G1, CAP <218, degree of steatosis <11 %; G2, 218 ≤ CAP <256, 11 % ≤ degree of steatosis <34 %; G3, 256 ≤ CAP <292, 11 % ≤ degree of steatosis <34 %; and G4, CAP >292, degree of steatosis ≥67 %) [24].

2.3. MRI-PDFF measurement

Participants underwent MRI-PDFF examination of the livers using a 3.0 T MRI scanner (Ingenia, Philips Healthcare, Best, Netherlands) with scan sequence mDIXON-Quant. The scanning range was full liver volume from the top of the diaphragm to the lower edge of the liver. Scanning parameters included the following: repetition time, 9.1 ms; echo time, 1.33 ms; gradient echo, 6; echo interval time, 1.3 ms; field-of-view, 180 mm × 140 mm; flip angle, 3°; resolution, 2.5 mm × 2.5 mm × 3.0 mm; and scan time, 12.5s. After scanning, the original images were transmitted to a workstation (IntelliSpace Portal, Philips Healthcare, Best, Netherlands), automatically generating water, fat, fat fraction, R2*, and T2* images.

The results were analyzed by a radiologist with >5 years of MR diagnostic experience. In the MRI-PDFF image, the liver was divided into eight segments according to the Couinaud liver segment division method, and one region of interest (ROI) was selected for measurement. The ROI was located in the liver parenchyma, avoiding the bile duct and vascular and extrahepatic structures, and the average value of the nine ROIs was defined as liver fat content. Additionally, participants were grouped based on MRI-PDFF values, as

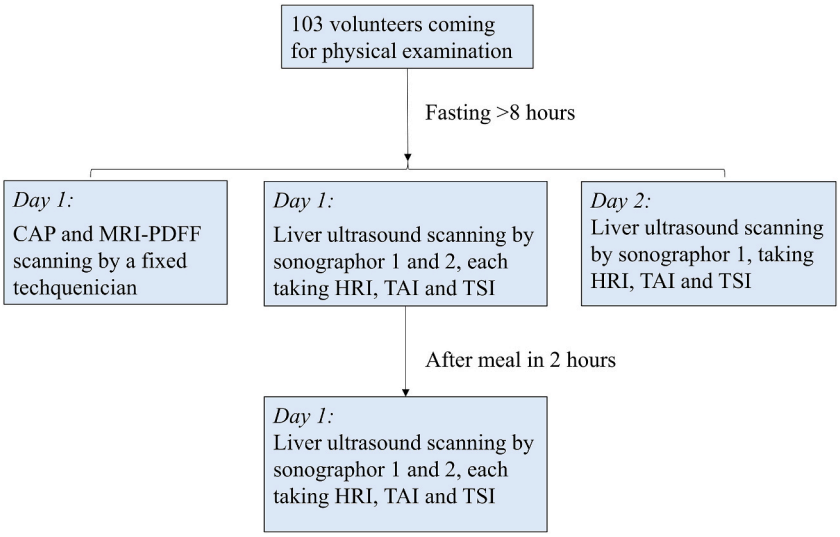

Fig. 1. Flow chart of the study design.
Note: CAP, controlled attenuation parameter; MRI-PDFF, magnetic resonance imaging-proton density fat fraction; TAI, tissue attenuation imaging; TSI, tissue scatter distribution imaging; HRI, hepatorenal index.

follows: M1, MRI-PDFF <5 %; M2, 5 % ≤ MRI-PDFF <10 %; and M3, MRI-PDFF ≥10 %) [25].

2.4. HRI, TAI and TSI measurement

B-mode liver US examination was performed using a US system (R10, Samsung Medison, Co., Ltd.) equipped with a convex CA1-7A probe by two radiologists (with ≥5 years' experience in abdominal US examinations) who were blinded to one another's results.

HRI data acquisition: Participants were positioned supine with the right arm maximally abducted. The operator placed the US probe near the right side of the subject' waist to obtain a standard section of the liver/kidney and "froze" it for HRI measurement. The system automatically identified the liver and kidney, selected the ROI, obtained grayscale values of the liver and kidney at the same sampling depth, and calculated the liver-kidney ratio (Fig. 2). Simultaneously, the operator could manually adjust the position of the ROI to select an ideal measurement area. HRI measurements were performed thrice, and the average was calculated.

TAI and TSI data acquisition: The participant remained in the same position and performed a slight breath-hold to obtain a stable image. The sonographer then acquired a view of S5 of the right liver from the intercostal window and pressed the "QUS" button on the touch screen where a set of time-gain compensations and positions of focus was fixed by the system, and the data at that time were recorded. A fan-shaped ROI, measuring 3 × 3 cm, was set according to the middle distance and fixed. The first ROI was placed at the midline of the entire image, with the upper edge of the ROI located 2 cm below the liver capsule. The operator pressed the "TAI" button to record the first TAI measurement and then pressed the "TSI" button to record the first TSI measurement. Subsequently, the operator placed the second ROI 4 cm below the superior hepatic capsule and recorded the two results. For the third measurement, the upper edge of the ROI was placed 6 cm below the liver capsule. Examples of quantitative US imaging, including TAI and TSI, are shown in Fig. 3a and b. The operator repeated the above process three times, calculating the average value of the ROI at each location.

2.5. Clinical and laboratory analysis

The operators used a digital scale to measure the height and weight of the participants, who removed their shoes and wore light clothes. Body mass index (BMI) was calculated as body weight (kg)/height, squared (m^2). Waist circumference was measured by the examiner using tape around the abdomen through the midpoint of the lower edge of the costal arch and the anterior superior spine. The participants then stood upright with their legs close together, and the tape was placed horizontally on the pubic symphysis and the most convex part of the gluteus maximus to measure hip circumference. The waist-to-hip ratio (WHR) was calculated using the following equation:

WHR = waist circumference (cm)/hip circumference (cm).

Venous blood samples were collected from all participants early in the morning after 8 h of fasting. All biochemical analyses were performed in the same laboratory using standard laboratory methods.

2.6. Statistical analyses

Normally distributed data are expressed as the mean (standard deviation), whereas data not normally distributed are expressed as the median (IQR). Comparisons between groups were performed using independent two-sample *t*-tests and non-parametric tests (Mann–Whitney *U* test). Pearson and Spearman correlation analyses were used to evaluate the correlation between continuous variables, and the intraclass correlation coefficient (ICC) was used to evaluate the repeatability of two measurements by the same operator and the consistency of the measurement results between different operators. The intra- and interobserver reliabilities of QUS measurements and the correlation between QUS and CAP or MRI-PDFF measurements were considered the primary outcomes. The sample size was calculated based on the assumption that the ICC for the QUS measurements had an effect size of at least 0.9 and that the correlation coefficient between the QUS and CAP measurements had an effect size >0.4. All sample size calculations assume two-sided analysis with a power of 90 % (1-β = 0.90) at a significance level of α = 0.05. With a dropout rate of approximately 10 %, a final sample

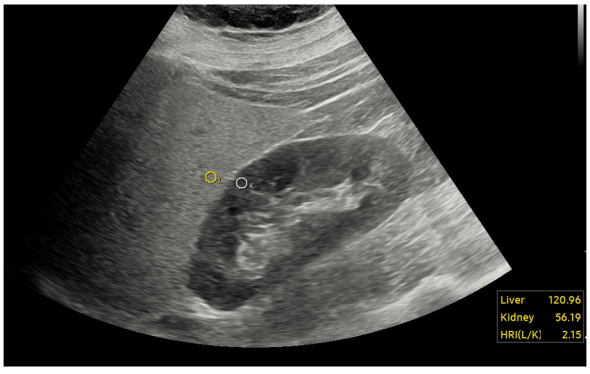

Fig. 2. Example of hepatorenal index (HRI) measurement.

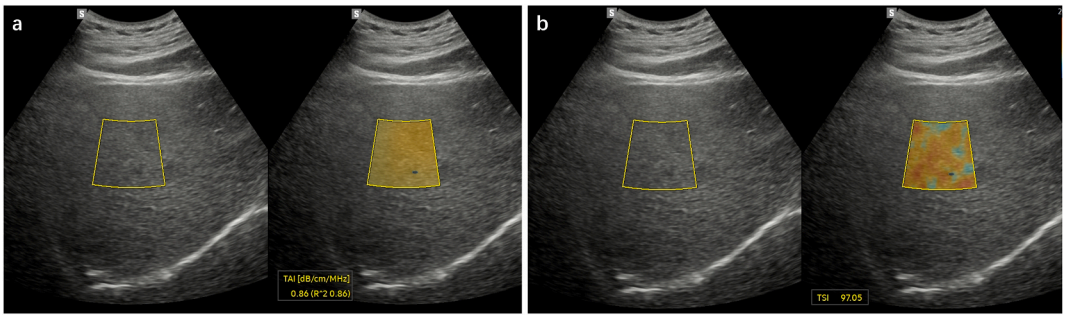

Fig. 3. Example of quantitative ultrasound imaging including TAI (a) and TSI (b). The upper edge of the region of interest is located 4 cm below the liver capsule.

size of 63 participants was needed. Although the sample size was not large, this study has clinical value as a methodological exploration. A p value < 0.05 was considered statistically significant. Statistical analyses were performed using SPSS version 26 (IBM Corporation, Armonk, NY, USA) and MedCalc version 20.0.3 (MedCalc Ltd, New York, NY, USA).

3. Results

3.1. Participant characteristics

A total of 103 participants (48 men [46.6 %], 55 women [53.3 %]; median age, 30.0 years [IQR 25.0–42.0 years]) were included in the study. The participants were all Asian, with a median BMI of 23.9 kg/m^2 (IQR 21.2–28.4 kg/m^2), including 51 (49.5 %) overweight or obese participants (BMI $\geq$24 kg/m^2). Demographic and clinical characteristics of the participants are summarized in Table 1.

Table 1
Characteristics of the study cohort.

Characteristics	Total (n = 103)
Sex, n (%)	
Male	48 (46.6 %)
Female	55 (53.3 %)
Age, median (IQR), y	30.0 (25.0, 42.0)
Height, median (IQR), cm	168.0 (160.0, 174.0)
Weight, median (IQR), kg	68.0 (58.0, 84.0)
BMI, median (IQR), kg/m^2	23.9 (21.2, 28.4)
WHR, mean (SD)	0.9 (0.8, 2.8)
TC, mean (SD), mmol/l	5.2 ± 0.8
TG, median (IQR), mmol/l	1.2 (0.7, 2.2)
LDL, mean (SD), mmol/l	3.1 ± 0.8
HDL, mean (SD), mmol/l	1.4 (1.1, 1.7)
AST, median (IQR), U/L	24.5 (19.8, 37.1)
ALT, median (IQR), U/L	23.3 (14.1, 50.1)
TBiL, mean (SD), μmol/L	12.8 (9.8, 16.2)
Albumin, mean (SD), g/L	48.0 ± 3.1
A/G, median (IQR)	1.6 (1.5, 1.8)
CAP, median (IQR), dB/m	228.0 (196.0258.0)
Dyslipidemia, n (%)	13 (12.6 %)
Hypertension, n (%)	9 (8.7 %)
Diabetes, n (%)	20 (19.4 %)

Normally distributed data were expressed as the mean ± standard deviation.
Data not normally distributed were expressed as the median and interquartile range.
Categorical variables were expressed as percentages.
BMI, body mass index; WHR, waist-to-hip ratio; TC, total cholesterol; TG, triglyceride; LDL, low-density lipoprotein; HDL, high-density lipoprotein; AST, aspartate aminotransferase; ALT, alanine aminotransferase; TBiL, total bilirubin; A/G, albumin/globulin; CAP, controlled attenuation parameter.

3.2. Effects of depth from the ROI to the liver capsule on TAI and TSI

Sixty-three participants underwent TAI and TSI examinations at different ROI depths. The operators sampled the upper (2 cm), middle (4 cm) and lower (6 cm) regions three times according to the depth of the ROI from the liver capsule. The results revealed that, with increasing depth, TAI measurements gradually decreased, whereas TSI measurements increased. The differences among the three sampling depths (Table 2) were significant. When obtaining TAI measurements, it was found that measurements from the upper (2 cm) region exhibited the strongest correlation with CAP measurements, whereas those from the middle (4 cm) region demonstrated a weaker correlation, and the correlation coefficient r remained >0.6. When obtaining TSI measurements, those from the middle (4 cm) region exhibited the strongest correlation with CAP measurements, whereas those from the upper (2 cm) region demonstrated a slightly weaker correlation with CAP measurements ($r > 0.6$). Measurements from the lower (6 cm) region were significantly less strongly correlated with CAP measurements ($r = 0.514$, $P < 0.0001$).

To further validate the diagnostic accuracy of QUS technology, TAI, TSI, and HRI measurements were compared with the MRI-PDFF results of another 40 participants (Table 3). The results revealed a significant positive correlation between TAI and MRI-PDFF measurements ($r = 0.753$, $P < 0.0001$). Moreover, TAI results among the three levels of MRI-PDFF (M1 < 5 %; 5 % ≤ M2 <10 %; M3 ≥ 10 %) were statistically different, and as the grading of MRI-PDFF increased, TAI increased sequentially (Fig. 4a–c). The diagnostic efficacy of TAI for different degrees of MRI-PDFF is presented in Fig. 4d. The correlation of TSI and HRI with MRI-PDFF was not significant. However, the sample size of the newly enrolled group was relatively small, and the research results still need further validation.

3.3. Effect of fasting or not on TAI, TSI and HRI measurements

Measurements from the participants were obtained in the fasting and postprandial states twice, and the results demonstrated no significant differences in the TAI, TSI, and HRI measurements between the two states (Table 2). Regardless of state (i.e., fasting or postprandial), TAI and TSI results from ROIs located in the upper and middle regions were significantly better than those from ROIs in the lower region. With increasing CAP grade, TAI and TSI demonstrated a consistent increasing trend (Fig. 5a–d). However, HRI measurements were less strongly correlated with CAP grade in either the fasted or postprandial state.

3.4. Intra- and interoperator reproducibility evaluation

The same operator obtained measurements twice on different days, and the results demonstrated good consistency for both TAI and TSI measurements but poor consistency for HRI measurements. The ICC was >0.9 for TAI regardless of whether the ROI was located in the upper, middle or lower regions. The ICC was >0.8 for TSI in the upper and middle regions but was significantly lower (0.681) in the deep region. The ICC for HRI measurements obtained twice by the same operator on different days was only 0.458.

The consistency measurements, independently obtained by the two operators,were good for both TAI and TSI but poor for HRI. The ICC was >0.8 for TAI regardless of whether the measurements were obtained from the upper, middle, or lower region. The ICC was >0.7 for TSI in the upper and middle regions but was significantly lower (0.622) in the deep region. The ICC for HRI was 0.343 for the two operators (Table 4).

4. Discussion

We analyzed new QUS techniques, including TAI, TSI, and HRI, to quantitatively assess the severity of fatty liver disease. Some studies have evaluated the feasibility and repeatability of this QUS technology; however, unified operational specifications remain lacking. Therefore, this study attempted to design a relatively comprehensive scheme to determine the most reliable measurement standard, thereby providing a reference for the standardized clinical application of QUS.

In practical clinical practice, we found that different ROI localizations in the QUS technique affected the accuracy of the measured

Table 2
Exploration of influencing factors of TAI, TSI and HRI measurement and their correlation with CAP.

Characteristics	ROI location	Determination			Correlation analysis with CAP (r)
		Fasting	2h after a meal	P value	
TAI	the upper (2 cm)	0.7 (0.7, 0.8)	0.7 (0.7, 0.8)	>0.05	0.650
	the middle (4 cm)	0.7 (0.6, 0.7)	0.7 (0.6, 0.7)	>0.05	0.607
	the lower (6 cm)	0.6 (0.6, 0.7)	0.6 (0.6, 0.7)	>0.05	0.587
TSI	the upper (2 cm)	78.3 ± 10.1	78.7 ± 10.3	>0.05	0.630
	the middle (4 cm)	82.3 ± 11.5	82.7 ± 11.8	>0.05	0.653
	the lower (6 cm)	90.0 ± 11.2	90.5 ± 10.7	>0.05	0.514
HRI		1.6 ± 0.4	1.5 ± 0.4	>0.05	0.281

Normally distributed data were expressed as the mean ± standard deviation.
Data not normally distributed were expressed as the median and interquartile range.
TAI, tissue attenuation imaging; TSI, tissue scatter distribution imaging; HRI, hepatorenal index; CAP, controlled attenuation parameter; ROI, region of interest.

Table 3
Exploration of the correlation between TAI, TSI, HRI and MRI-PDFF.

Characteristics	mean (SD)	Correlation analysis with MRI-PDFF (r)	P value
TAI	0.9 ± 0.2	0.753	<0.0001
TSI	94.8 ± 4.5	0.064	>0.05
HRI	2.8 ± 1.1	0.371	>0.05

Normally distributed data were expressed as the mean ± standard deviation.
Data not normally distributed were expressed as the median and interquartile range.
MRI-PDFF, magnetic resonance imaging proton density fat fraction; TAI, tissue attenuation imaging; TSI, tissue scatter distribution imaging; HRI, hepatorenal index.

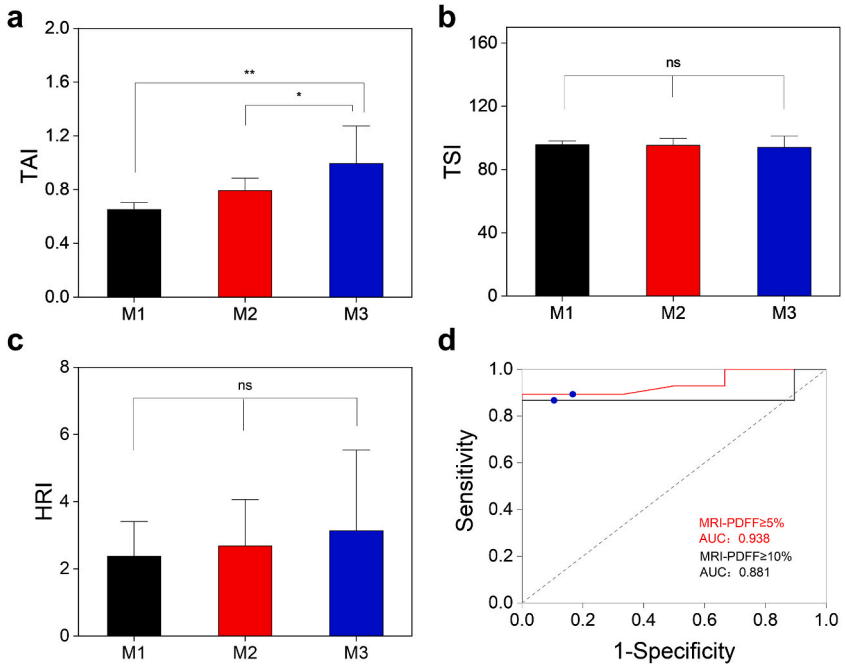

Fig. 4. Changes of TAI, TSI and HRI under different MRI-PDFF grades.
(M1, MRI-PDFF <5 %; M2, 5 % ≤ MRI-PDFF <10 %; and M3, MRI-PDFF ≥10 %)
Changes in TAI mean values under different MRI-PDFF levels.
(a) Changes in TSI mean values under different MRI-PDFF levels
(b) Changes in HRI mean values under different MRI-PDFF levels
(c) ROC curve analysis for TAI classification of MRI-PDFF ≥5 % (red) and ≥10 % (black).
Note: TAI, tissue attenuation imaging; TSI, tissue scatter distribution imaging; HRI, hepatorenal index; ROC, receiver operating characteristic curve; AUC, area under the receiver operating characteristic curve; MRI-PDFF, magnetic resonance imaging-based proton density fat fraction measurement. (For interpretation of the references to colour in this figure legend, the reader is referred to the Web version of this article.)

results. Kang et al. fixed the sampling depth in the range of 4–8 cm and evaluated the accuracy of QUS in diagnosing NAFLD based on pathology [15]. The results suggested excellent performance; however, the repeatability of the measurement results was not evaluated. In our study, we found a significant difference in the measurement results in the 4–8 cm depth range. Similarly, Jeon et al. [26] and Rónaszéki et al. [13] evaluated the diagnostic performance and reproducibility of QUS at sampling depths >2 cm and >3 cm, respectively, and demonstrated good measurement results; however, the sampling depth range was too wide, and there was no clear operating standard to regulate the process. However, in the ROI comparison study by Sugimoto et al. [27], the best diagnostic accuracy for fatty liver was obtained when the sampling depth was at least two times the liver capsule depth, which is different from our findings. Theoretically, the AC values of the same homogeneous liver tissues should be the same, with more severe fat infiltration yielding higher AC values. From the overall attenuation and scattering trend, the TAI measurements increased with increasing sampling depth, whereas the TSI measurements decreased with increasing sampling depth. We believe that this difference is related to the measurement error of this technology with increasing depth.

When unreliable measurements at deeper locations were excluded, we found a high reproducibility of measurements within and between groups for TAI and TSI. In clinical practice, different physicians use different operating techniques and select different US slices and ROI positions, which may lead to incomplete measurement results. However, if examinations are performed according to a uniform operating standard, good repeatability can be achieved for the same patient of different operators, which is the basis for the

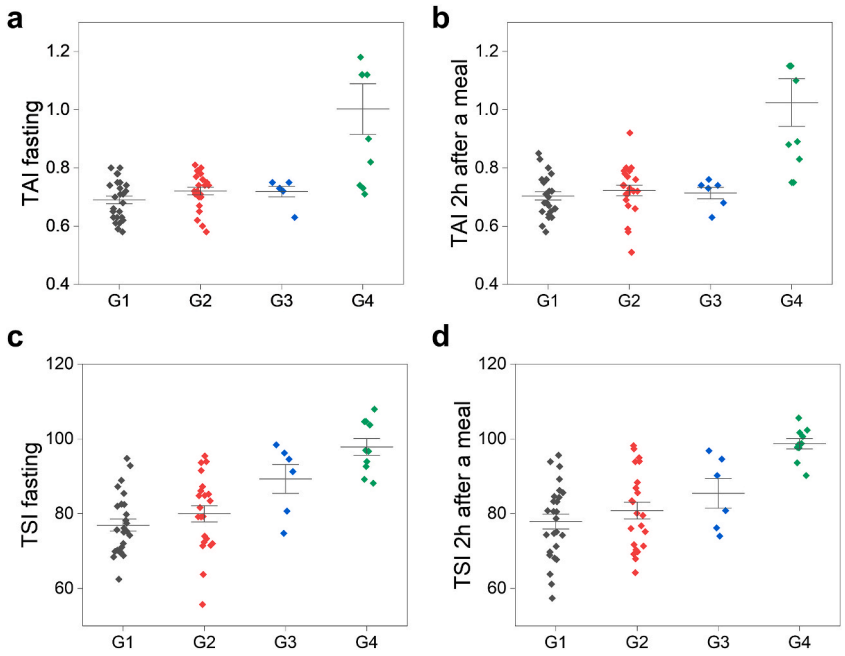

Fig. 5. Changes of TAI and TSI under different CAP grades.
(**< 218** (degree of hepatic steatosis <11 %); **≥ 218, < 256** (11 % ≤degree of hepatic steatosis <34 %); **≥ 256, < 292** (34 % ≤ degree of hepatic steatosis <67 %); **≥ 292** (degree of hepatic steatosis ≥67 %))
(a) Changes of TAI under different CAP grades in fasting.
(b) Changes of TAI under different CAP grades during 2 h after meal.
(c) Changes of TSI under different CAP grades in fasting.
(d) Changes of TSI under different CAP grades during 2 h after meal.
Note: CAP, controlled attenuation parameter; TAI, tissue attenuation imaging; TSI, tissue scatter distribution imaging.

Table 4
Intra- and inter-observer reliability of TAI, TSI and HRI.

Intra-class correlation coefficient	TAI			TSI			HRI
	the upper	the middle	the lower	the upper	the middle	the lower	
Intra-observer reliability	0.931	0.933	0.920	0.925	0.806	0.681	0.458
Inter-observer reliability	0.894	0.896	0.884	0.766	0.709	0.622	0.343

TAI, tissue attenuation imaging; TSI, tissue scatter distribution imaging; HRI, hepatorenal index.

clinical application of this technology.

The HRI is based on the ratio of the grayscale of the liver parenchyma to that of the renal cortex, calculated in B mode. Previous studies have shown that HRI is related to various factors, such as instrument setup, total gain, time gain compensation, focus position, and ROI sampling position. Although we attempted to control for the above parameters to be consistent, compared with the visual qualitative analysis of liver and kidney echo differences, such a quantitative evaluation method has a lower reliability. It may be that the different "ideal" liver and kidney sections obtained each time were different, and on such sections, the grayscale values of the liver parenchyma and renal cortex sampling sites were also different, resulting in poor repeatability of each measurement [28].

Currently, most researchers believe that liver congestion and elevated liver enzyme and bilirubin levels may lead to false-positive results. Therefore, fasting for >8 h is usually recommended for general abdominal US examinations. However, some studies have found no significant differences with or without fasting, and this result has also been reported in studies investigating CAP and other TAI-like measurements [16,29]. The impact of fasting on the measurement results remains inconclusive. Although this exploratory study found no differences in the results, the mechanism has not been explored further. In the future, more in-depth research is required to formulate a unified operating standard.

The innovation of this prospective study lies in its methodological exploration and multidimensional comparison to determine the best standard for QUS measurement and evaluate its accuracy and repeatability. The design of the research protocol was relatively comprehensive. Considering that there is currently no unified measurement standard for these new techniques in clinical practice, this study has practical clinical value and reference significance.

This study had several limitations, the first of which was its single-center design and relatively small sample size. Although the

research design was relatively comprehensive, the results of this study need to be further verified in a large-scale, multicenter cohort study. Second, this study lacked histological reference standards. The grading accuracy of the CAP as the "ground truth" needs to be studied. Although it has shown promising results in quantifying hepatic steatosis, a consensus regarding the optimal cutoffs and diagnostic grading ability is unavailable. The optimal cutoff points for CAP depend substantially on aetiology [30]. Although MRI methods can accurately estimate total liver fat, which is valuable in clinical research, they are not ideal for screening large, at-risk populations. This highlights the urgent need for alternative non-invasive examination methods.

5. Conclusion

This study evaluated the reliability of new QUS techniques for diagnosing hepatic steatosis in multiple dimensions and explored the optimal measurement criteria for these methods. Since a unified measurement standard has not yet been formed for these new techniques in clinical practice, this study has certain clinical practical value and reference significance. However, in the future, large-sample multicenter studies are needed for further verification and improvement to establish unified operating specifications and diagnostic criteria.

Funding

The work was supported by the National Key R&D Program [2021YFC2009100], Shanghai Science and Technology Commission [21Y11910900], and Shanghai Sixth People's Hospital Surface Cultivation Project [ynms202110]. Tongji University Affiliated Tongji Hospital Project [GJPY2318, RCQD2401].

Ethics statement

This study was reviewed and approved by ethics committee of Shanghai Sixth People's Hospital Affiliated to Shanghai Jiao Tong University School of Medicine, with the approval number: [2021-KY-025(K)]. All participants/patients provided informed consent to participate in the study.

Data availability statement

Data associated with the study has not been deposited into a publicly available repository. Data are available from the corresponding author on reasonable request.

CRediT authorship contribution statement

Xiao Li: Writing – review & editing, Writing – original draft, Formal analysis, Data curation, Conceptualization. **Ziwei Sun:** Writing – original draft, Formal analysis, Data curation. **Wei Liu:** Methodology, Investigation, Formal analysis. **Lianjie Sun:** Writing – review & editing, Methodology, Conceptualization. **Junyi Ren:** Validation, Supervision. **Ying Xu:** Writing – original draft, Visualization, Validation. **Haoyong Yu:** Writing – review & editing, Conceptualization. **Wenkun Bai:** Writing – review & editing, Funding acquisition, Conceptualization.

Declaration of competing interest

The authors declare that they have no known competing financial interests or personal relationships that could have appeared to influence the work reported in this paper.

Acknowledgments

The authors would like to express their gratitude for the contribution of all trial participants.

References

[1] J.V. Lazarus, P.N. Newsome, S.M. Francque, F. Kanwal, N.A. Terrault, M.E. Rinella, Reply: a multi-society Delphi consensus statement on new fatty liver disease nomenclature, Hepatology 79 (3) (2024) E93–E94, https://doi.org/10.1097/HEP.0000000000000696.
[2] S. McPherson, T. Hardy, E. Henderson, et al., Evidence of NAFLD progression from steatosis to fibrosing-steatohepatitis using paired biopsies: implications for prognosis and clinical management, J. Hepatol. 62 (5) (2015) 1148–1155, https://doi.org/10.1016/j.jhep.2014.11.034.
[3] P. Angulo, D.E. Kleiner, S. Dam-Larsen, et al., Liver fibrosis, but No other histologic features, is associated with long-term outcomes of patients with nonalcoholic fatty liver disease, Gastroenterology 149 (2) (2015) 389, https://doi.org/10.1053/j.gastro.2015.04.043, 97.e10.
[4] C. Caussy, S.B. Reeder, C.B. Sirlin, R. Loomba, Noninvasive, quantitative assessment of liver fat by MRI-PDFF as an endpoint in NASH trials, Hepatology 68 (2) (2018) 763–772, https://doi.org/10.1002/hep.29797.
[5] L. Castera, M. Friedrich-Rust, R. Loomba, Noninvasive assessment of liver disease in patients with nonalcoholic fatty liver disease, Gastroenterology 156 (5) (2019) 1264–1281.e4, https://doi.org/10.1053/j.gastro.2018.12.036.
[6] T. Karlas, D. Petroff, M. Sasso, et al., Individual patient data meta-analysis of controlled attenuation parameter (CAP) technology for assessing steatosis, J. Hepatol. 66 (5) (2017) 1022–1030, https://doi.org/10.1016/j.jhep.2016.12.022.

[7] K.Q. Shi, J.Z. Tang, X.L. Zhu, et al., Controlled attenuation parameter for the detection of steatosis severity in chronic liver disease: a meta-analysis of diagnostic accuracy, J. Gastroenterol. Hepatol. 29 (6) (2014) 1149–1158, https://doi.org/10.1111/jgh.12519.
[8] H.N. Şendur, M.N. Cerit, N. Ibrahimkhanli, A.B. Şendur, S. Özhan Oktar, Interobserver variability in ultrasound-based liver fat quantification, J. Ultrasound Med. 42 (4) (2023) 833–841, https://doi.org/10.1002/jum.16048.
[9] S.K. Jeon, J.M. Lee, I. Joo, Feasibility of quantitative ultrasound imaging for suspected hepatic steatosis: intra- and inter-examiner reliability and correlation with controlled attenuation parameter, Ultrasound Med. Biol. 47 (3) (2021) 438–445, https://doi.org/10.1016/j.ultrasmedbio.2020.11.009.
[10] S.K. Jeon, I. Joo, S.Y. Kim, et al., Quantitative ultrasound radiofrequency data analysis for the assessment of hepatic steatosis using the controlled attenuation parameter as a reference standard, Ultrasonography 40 (1) (2021) 136–146, https://doi.org/10.14366/usg.20042.
[11] S.K. Jeon, J.M. Lee, I. Joo, et al., Quantitative ultrasound radiofrequency data analysis for the assessment of hepatic steatosis in nonalcoholic fatty liver disease using magnetic resonance imaging proton density fat fraction as the reference standard, Korean J. Radiol. 22 (7) (2021) 1077–1086, https://doi.org/10.3348/kjr.2020.1262.
[12] D.I. Cha, T.W. Kang, J.H. Min, et al., Deep learning-based automated quantification of the hepatorenal index for evaluation of fatty liver by ultrasonography, Ultrasonography 40 (4) (2021) 565–574, https://doi.org/10.14366/usg.20179.
[13] A.D. Rónaszéki, B.K. Budai, B. Csongrády, et al., Tissue attenuation imaging and tissue scatter imaging for quantitative ultrasound evaluation of hepatic steatosis, Medicine (Baltim.) 101 (33) (2022) e29708, https://doi.org/10.1097/MD.0000000000029708.
[14] Y.L. Huang, H. Bian, Y.L. Zhu, et al., Quantitative diagnosis of nonalcoholic fatty liver disease with ultrasound attenuation imaging in a biopsy-proven cohort [published online ahead of print, 2023 jul 3], Acad. Radiol. S1076–6332 (23) (2023) 288–X, https://doi.org/10.1016/j.acra.2023.05.033.
[15] K.A. Kang, S.R. Lee, D.W. Jun, I.G. Do, M.S. Kim, Diagnostic performance of a novel ultrasound-based quantitative method to assess liver steatosis in histologically identified nonalcoholic fatty liver disease, Med Ultrason 25 (1) (2023) 7–13, https://doi.org/10.11152/mu-3815.
[16] M. Silva, P. Costa Moreira, A. Peixoto, et al., Effect of meal ingestion on liver stiffness and controlled attenuation parameter, GE Port. J. Gastroenterol. 26 (2) (2019) 99–104, https://doi.org/10.1159/000488505.
[17] K. Ratchatasettakul, S. Rattanasiri, K. Promson, P. Sringam, A. Sobhonslidsuk, The inverse effect of meal intake on controlled attenuation parameter and liver stiffness as assessed by transient elastography, BMC Gastroenterol. 17 (1) (2017) 50, https://doi.org/10.1186/s12876-017-0609-6. Published 2017 Apr 13.
[18] Expert Panel on Detection, Evaluation, Treatment of high blood cholesterol in adults. Executive summary of the third report of the national cholesterol education Program (NCEP) expert Panel on detection, evaluation, and treatment of high blood cholesterol in adults (Adult treatment Panel III), JAMA 285 (19) (2001) 2486–2497, https://doi.org/10.1001/jama.285.19.2486.
[19] B. Williams, G. Mancia, W. Spiering, et al., 2018 ESC/ESH Guidelines for the management of arterial hypertension, Eur. Heart J. (39) (2018) 3021–3104, https://doi.org/10.1093/eurheartj/ehy339 [published correction appears in Eur Heart J. 2019 Feb 1;40(5):475].
[20] American Diabetes Association, 2. Classification and diagnosis of diabetes: standards of medical care in diabetes-2019, Diabetes Care (42) (2019) S13–S28, https://doi.org/10.2337/dc19-S002.
[21] I. Mikolasevic, L. Orlic, N. Franjic, et al., Transient elastography (FibroScan(®)) with controlled attenuation parameter in the assessment of liver steatosis and fibrosis in patients with nonalcoholic fatty liver disease - where do we stand? World J. Gastroenterol. 22 (32) (2016) 7236–7251, https://doi.org/10.3748/wjg.v22.i32.7236.
[22] H. Garg, SShalimar Aggarwal, et al., Utility of transient elastography (fibroscan) and impact of bariatric surgery on nonalcoholic fatty liver disease (NAFLD) in morbidly obese patients, Surg. Obes. Relat. Dis. 14 (1) (2018) 81–91, https://doi.org/10.1016/j.soard.2017.09.005.
[23] S. Oeda, K. Tanaka, A. Oshima, et al., Diagnostic accuracy of FibroScan and factors affecting measurements, Diagnostics 10 (11) (2020) 940, https://doi.org/10.3390/diagnostics10110940.
[24] V. de Lédinghen, J. Vergniol, J. Foucher, W. Merrouche, B. le Bail, Non-invasive diagnosis of liver steatosis using controlled attenuation parameter (CAP) and transient elastography, Liver Int. 32 (6) (2012) 911–918, https://doi.org/10.1111/j.1478-3231.2012.02820.x.
[25] European Association for the Study of the Liver (EASL); European Association for the Study of Diabetes (EASD); European Association for the Study of Obesity (EASO), EASL-EASD-EASO Clinical Practice Guidelines for the management of non-alcoholic fatty liver disease, J. Hepatol. 64 (6) (2016) 1388–1402, https://doi.org/10.1016/j.jhep.2015.11.004.
[26] S.K. Jeon, J.M. Lee, I. Joo, Clinical feasibility of quantitative ultrasound imaging for suspected hepatic steatosis: intra- and inter-examiner reliability and correlation with controlled attenuation parameter, Ultrasound Med. Biol. 47 (3) (2021) 438–445, https://doi.org/10.1016/j.ultrasmedbio.2020.11.009.
[27] K. Sugimoto, M. Abe, H. Oshiro, et al., The most appropriate region-of-interest position for attenuation coefficient measurement in the evaluation of liver steatosis, J. Med. Ultrason. 48 (4) (2001) 615–621, https://doi.org/10.1007/s10396-021-01124-z, 2021.
[28] S. Srigandan, M. Zelesco, S. Abbott, et al., Correlation between hepatorenal index and attenuation imaging for assessing hepatic steatosis, Australas J Ultrasound Med 25 (3) (2022) 107–115, https://doi.org/10.1002/ajum.12297.
[29] Y. Zhao, M. Jia, C. Zhang, et al., Reproducibility of ultrasound-guided attenuation parameter (UGAP) to the noninvasive evaluation of hepatic steatosis, Sci. Rep. 12 (1) (2022) 2876, https://doi.org/10.1038/s41598-022-06879-0.
[30] D. Petroff, V. Blank, P.N. Newsome, et al., Assessment of hepatic steatosis by controlled attenuation parameter using the M and XL probes: an individual patient data meta-analysis, Lancet Gastroenterol Hepatol 6 (3) (2021) 185–198, https://doi.org/10.1016/S2468-1253(20)30357-5.